Surface Modes and Ordered Patterns during Spinodal Decomposition of an *ABv* Model Alloy

Mathis Plapp and Jean-François Gouyet
Laboratoire de Physique de la Matière Condensée, Ecole Polytechnique, 91128 Palaiseau cedex, France
(Received 28 January 1997)

We study a lattice gas model for a binary alloy with vacancies by means of a mean-field kinetic equation. Simulations of droplets of unstable mixture immersed in a stable vapor show the emergence of ordered structures at the surface which propagate into the bulk. We calculate characteristic wavelengths and propagation velocities of these patterns by a linear stability analysis. The thickness of the ordered layer depends on the model parameters and the strength of the initial noise. [S0031-9007(97)03364-4]

PACS numbers: 64.75.+g, 05.70.Ln, 64.60.Cn, 68.35.Rh

Spinodal decomposition [1,2] takes place when a mixture or alloy is rapidly quenched into a thermodynamically unstable state. Long-wavelength concentration fluctuations are amplified to form a complicated domain pattern which then coarsens. Whereas this process is well understood in the bulk of crystals or fluids, recently surface effects on spinodal decomposition were investigated in polymer and fluid systems [3–7]. If a surface prefers energetically one of the components of the mixture, a wetting layer is rapidly formed, and an oscillating concentration profile propagates into the interior of the mixture. In some cases, lateral structures are formed at the surface which coarsen much more rapidly than in the bulk [4]. The formation of these structures depends on the wetting properties of the involved surfaces [6].

The theoretical work includes Monte Carlo simulations [8,9], investigations based on phenomenological Ginzburg-Landau equations [10–13], and studies of a model system by a mean-field kinetic equation [14]. Attention was drawn recently to the modification of interface structures during the spinodal decomposition process [12], and to the occurrence of surface modes [13] in an unstable mixture in contact with a substrate surface. Some of these modes grow faster than the ordinary bulk modes and create periodic structures along the surface.

We want to report here about similar findings in the dynamics of a simple lattice gas model of a binary alloy with vacancies. Such models were investigated by several authors [15–18], motivated by the fact that a vacancy mechanism is a more realistic picture of diffusion in solids than the more widely used exchange model. Here, we study interfaces between an unstable mixture and a stable vapor phase. Such interfaces are created when one quenches a small droplet of a stable mixture in a bath of vapor into an unstable region of the phase diagram. Decomposition at the surface is triggered by instabilities in the interface and competes with the decomposition in the bulk.

Our model is based on a stochastic lattice gas. A two-dimensional quadratic lattice with N sites and periodic boundary conditions is occupied by atoms of two species A and B, and by vacancies v. Multiple occupation is forbidden, and we define the occupation numbers at each site i, n_i^A, n_i^B, and $n_i^v \in \{0, 1\}$, with $n_i^A + n_i^B + n_i^v = 1\ \forall i$. The Hamiltonian is

$$H = -\varepsilon_{AA} \sum_{\langle i,j \rangle} n_i^A n_j^A - \varepsilon_{BB} \sum_{\langle i,j \rangle} n_i^B n_j^B - \varepsilon_{AB} \sum_{\langle i,j \rangle} (n_i^A n_j^B + n_i^B n_j^A), \quad (1)$$

where ε_{AA}, ε_{BB}, and ε_{AB} are the interaction energies between A and B atoms, the sums are over all pairs of nearest neighbors, and we have chosen the Ising convention: An attractive interaction is positive. The atoms can exchange places only with a vacancy. We assume these jumps to be activated processes, and their rates to follow an Arrhenius law, as often observed in metallic diffusion. The activation energy is given by the local binding energy, which leads to jump rates from site i to a neighboring site j:

$$w_{ij}^{\alpha} = w_0^{\alpha} \exp\left(-\beta \varepsilon_{\alpha A} \sum_a n_{i+a}^A - \beta \varepsilon_{\alpha B} \sum_a n_{i+a}^B \right), \quad (2)$$

where β is the inverse of temperature (constant throughout the system), the sums are over the nearest-neighbor sites of the start site, and α stands for A or B. w_0^{α} are attempt frequencies. We will consider only the case $w_0^B = w_0^A = w_0$. In the following, we will measure all lengths in units of the lattice constant a and time in units of w_0^{-1}. The transition rates (2) satisfy detailed balance and thus lead to the correct equilibrium state in the infinite time limit.

The evolution of such a nonequilibrium system can be described by the master equation for the time-dependent probability distribution in the space of configurations. If we define by angular brackets the average with respect to this distribution, we can write evolution equations for the local occupation probabilities $p_i^A = \langle n_i^A \rangle$ and $p_i^B = \langle n_i^B \rangle$, which can be interpreted as concentrations as well. We allow only nearest-neighbor jumps, and find

$$\frac{dp_i^{\alpha}}{dt} = -\sum_a j_{i,i+a}^{\alpha}, \quad (3)$$

 0031-9007/97/78(26)/4970(4)$10.00

where $j^{\alpha}_{i,i+a}$ is the current of species α in the link $(i, i+a)$, given by

$$j^{\alpha}_{i,j} = \langle n^{\alpha}_i (1 - n^A_j - n^B_j) w^{\alpha}_{ij} - n^{\alpha}_j (1 - n^A_i - n^B_i) w^{\alpha}_{ji} \rangle . \tag{4}$$

The factors multiplying the transition rates ensure that the start site is occupied by an atom of species α, the target site by a vacancy. We have $p^v_i = 1 - p^A_i - p^B_i$, and thus two independent variables per site.

We now make a mean-field approximation: We replace the occupation numbers in (4) by their averages, thus neglecting all correlations. Similar equations have been used to describe phase separation in alloys [14,18–21] and dendritic growth [22]. The equations (4) can be cast in a form more closely related to out-of-equilibrium thermodynamics. Simple rearrangements yield

$$j^{\alpha}_{ij} = -M^{\alpha}_{ij} (\mu^{\alpha}_j - \mu^{\alpha}_i) , \tag{5}$$

where

$$M^{\alpha}_{ij} = (1 - p^A_i - p^B_i)(1 - p^A_j - p^B_j) \times (e^{\beta \mu^{\alpha}_j} - e^{\beta \mu^{\alpha}_i})/(\mu^{\alpha}_j - \mu^{\alpha}_i) \tag{6}$$

is the atomic mobility of species α in the link ij and

$$\mu^{\alpha}_i = -\varepsilon_{\alpha A} \sum_a (p^A_{i+a} - p^A_i) - \varepsilon_{\alpha B} \sum_a (p^B_{i+a} - p^B_i) + -z\varepsilon_{\alpha A} p^A_i - z\varepsilon_{\alpha B} p^B_i + \beta^{-1} \ln[p^{\alpha}_i/(1 - p^A_i - p^B_i)] \tag{7}$$

is the local chemical potential of species α. Here, z is the coordination number of the lattice ($z = 4$ for our square lattice). These chemical potentials are the derivatives with respect to the local concentrations p^{α}_i of a free energy F which has the form of a discrete Ginzburg-Landau functional. The free energy density f is the same as obtained by standard static mean-field theory. At equilibrium, all time derivatives vanish and the chemical potentials are constant throughout the system.

Equations (3) and (5) have the structure of a generalized Cahn-Hilliard equation [1]. However, there are two conserved local order parameters, and the phase diagram is more complex than for a binary mixture. It can be obtained from the free energy density f. Stability in the binary subsystems Av, Bv, and AB is controlled by ε_{AA}, ε_{BB}, and $\varepsilon = \varepsilon_{AA} + \varepsilon_{BB} - 2\varepsilon_{AB}$, respectively. If all these energies are positive, we always find three-phase coexistence of an A-rich, a B-rich, and a vacancy-rich "vapor" phase at sufficiently low temperatures. Evidently, in a real vapor, diffusion does not take place by activated nearest-neighbor jumps. The important property of this phase is that diffusion is much faster than in the "solid." As we focus here on the dynamics inside the solid, the details of the diffusion mechanism in the vapor are of little importance. As a specific example, we choose $\varepsilon_{AA} = \varepsilon_{BB}$ and $\varepsilon_{AB} = \varepsilon_{AA}/2$. Then, we have $\varepsilon = \varepsilon_{AA} = \varepsilon_{BB}$, and the phase diagram is completely symmetric.

We immersed a droplet of initial radius $R = 55$ and concentrations $p^A = p^B = 0.46464$ in a vapor of concentration $p^A = p^B = 0.03536$ and fixed the temperature to have $\beta\varepsilon_{AA} = 2$. Then, we have equal pressure and chemical potentials in the two phases (the pressure P is defined as the negative of the grand potential $P = -f + \mu_A p^A + \mu_B p^B$). Note that as long as $p^A = p^B$ in both phases, the vapor-mixture interface is "neutral." Such an initial condition cannot be chosen in a simple Ising model without vacancies or in the standard Cahn-Hilliard equation, because in binary systems any stable phase below the critical temperature will prefer either A or B. We added a random noise of small amplitude over the whole system to initialize the phase separation and integrated the mean-field equations using a simple Euler algorithm. Phase separation shows up first at the surface, giving a regularly modulated structure along the boundary of the droplet (Fig. 1). This surface mode propagates into the droplet, leaving behind a checkerboardlike structure,

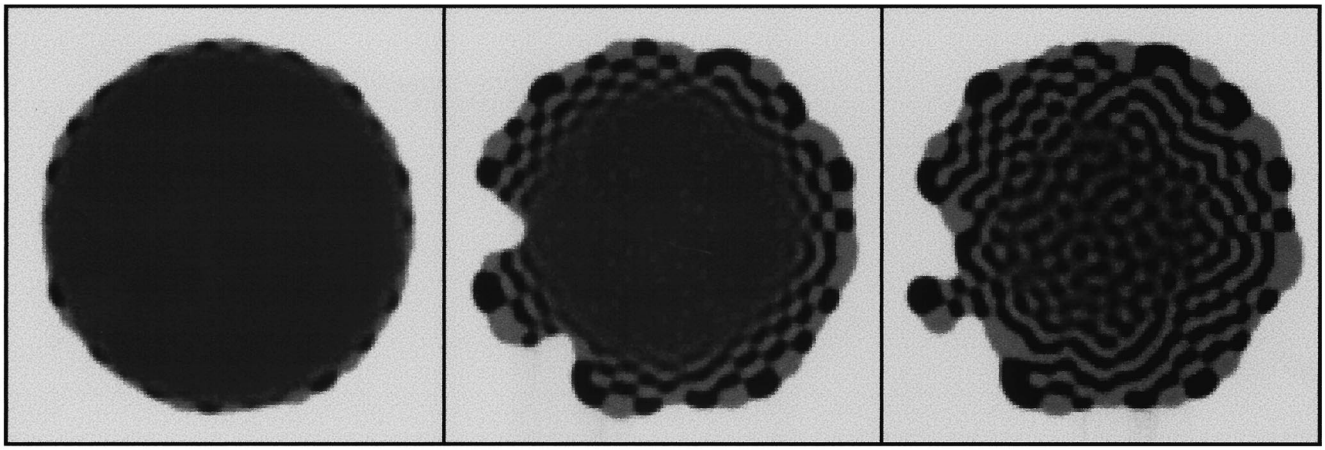

FIG. 1. Snapshot pictures at $t = (22\,400,\ 56\,900,$ and $79\,400) w_0^{-1}$ (from left to right) of a decomposing droplet on a 128×128 lattice. White: vapor; black: A-rich; light grey: B-rich phase; dark grey: mixture. Parameter values as given in the text.

which coalesces rather rapidly to form stripes. At the same time, fingers of vapor penetrate into the mixture. This is an instability of Mullins-Sekerka-type [23] which is driven by the diffusion of vacancies out of the solid. The fingers stop to grow once a layer of fully decomposed material has formed along their entire boundary and are smoothed out by the following coarsening processes. The propagation of the surface modes continues until the bulk modes have grown to a sufficiently big amplitude to enter the nonlinear regime of spinodal decomposition. We then find in the interior of the droplet the bicontinuous structures of bulk spinodal decomposition. At the surface, coarsening has proceeded much further than in the interior of the droplet. The initially smooth vapor-mixture interface has developed bulges. This is due to the existence of points at the surface where the three phases meet. At such points, local equilibrium fixes the angle between the *Av*, *Bv*, and *AB* interfaces.

This behavior was observed for several temperatures and various initial concentrations of vapor and mixture. It is due to a larger mobility of surface atoms. To check this assumption, we performed a linear stability analysis, which can only be sketched here. We must compare bulk and surface behavior. In the bulk, we start from a homogeneous state, that is $p_i^A = p^A$ and $p_i^B = p^B \ \forall i$, and add plane wave perturbations

$$\begin{pmatrix} p_j^A \\ p_j^B \end{pmatrix} = \begin{pmatrix} p^A \\ p^B \end{pmatrix} + \begin{pmatrix} \delta p^A \\ \delta p^B \end{pmatrix} \exp[i\vec{k} \cdot \vec{x}_j + \omega(\vec{k})t], \quad (8)$$

where $\vec{x}_j$ is the coordinate vector of site j, and $\vec{k} = (k_x, k_y)$ is the wave vector of the perturbation. Linearization of the equations of motion in δp^A and δp^B gives

$$\omega(\vec{k}) \begin{pmatrix} \delta p^A \\ \delta p^B \end{pmatrix} = A_{\vec{k}} \begin{bmatrix} M^A\,(-A_{\vec{k}}\varepsilon_{AA} + S_{AA}) & M^A\,(-A_{\vec{k}}\varepsilon_{AB} + S_{AB}) \\ M^B\,(-A_{\vec{k}}\varepsilon_{AB} + S_{AB}) & M^B\,(-A_{\vec{k}}\varepsilon_{BB} + S_{BB}) \end{bmatrix} \begin{pmatrix} \delta p^A \\ \delta p^B \end{pmatrix}. \quad (9)$$

Here, M^α are the limits of (6) for uniform chemical potentials, and S is the matrix of the second derivatives of the free energy density, $S_{\alpha\beta} = \partial^2 f / \partial p^\alpha \partial p^\beta$. $A_{\vec{k}}$ is given by the function

$$A_{\vec{k}} = -4 \sin^2(k_x/2) - 4 \sin^2(k_y/2). \quad (10)$$

The solution of the eigenvalue problem (9) gives the dispersion relations $\omega(\vec{k})$. The number of unstable branches is equal to the number of negative eigenvalues of S. For the example of Fig. 1, we have one negative eigenvalue, and the characteristic length scale of the bulk pattern is given by the maximum of the corresponding dispersion relation. We find a maximum growth rate of $\omega_b = 1.063 \times 10^{-4}$, with $|\vec{k}|$ near 1.

Now consider a vapor-mixture interface parallel to the y axis (directed along one of the lattice vectors). We can analyze the stability of the interface using Fourier modes in the y direction. However, instead of the two coefficients δp^A and δp^B we have to find the complete eigenmodes in the x direction, leading to an eigenvalue problem for a $2L_x \times 2L_x$ matrix, where L_x is the system size in the x direction. This is surely tractable using standard numerical methods, but we can limit ourselves here to a simpler treatment. We first calculate the profile resulting from the local equilibration of the initial step profile, solving the finite-difference equations $\mu_i^\alpha = \mu_{\text{bulk}}^\alpha$ through the interface. Then we isolate a small number of layers around the interface and perturb by Fourier modes along the y axis. If we take properly into account the corresponding boundary conditions, we can extract the dominating behavior from a much smaller matrix. The results do not depend on the number of layers as soon as we have included the whole interfacial region. Using the last two layers of vapor and the first two layers of solid, we find that only one branch of the resulting dispersion relation is unstable, with a maximum eigenvalue $\omega_s = 4.361 \times 10^{-4}$, at a value $k_y = 0.403$. The surface growth rate is four times larger than in the bulk, and the characteristic wave vector is very different. Initial conditions as the position and orientation of the vapor-mixture interface with respect to the lattice do not matter much, as we can see in the simulation: The wavelength of the surface mode is fairly regular.

Once a domain of A is formed on the surface, it attracts other A atoms from the solid, thus creating a depletion of A atoms giving rise to a B domain. Hence, the rapidly growing surface mode enforces growth with its proper growth rate and wave vector, which are different from the bulk values. We can get a first idea of the behavior in the bulk by inserting the surface growth rate ω_s and wave vector k_y in the bulk equations. Then (9) becomes a quadratic equation in $A_{\vec{k}}$ which has two complex roots. Using (10), we can solve for k_x and obtain the four solutions

$$k_x = \pm b \pm ic \quad (11)$$

with, in our case, $b = 1.05$ and $c = 0.789$. The two solutions to be kept are those with the positive imaginary part: They describe waves which decay exponentially with the penetration depth. They have a wavelength in the x direction of $\lambda_x = 2\pi/b$ and propagate with a velocity $v = \omega_s/c$. To test these predictions, we compared our findings to simulations in a stripe geometry. From simple inspection of these simulations we find $\lambda_y = 2\pi/k_y \approx 16$, $\lambda_x \approx 6$, and $v \approx 5 \times 10^{-4}$, whereas the predictions are 15.6, 5.73, and 5.32×10^{-4}.

Clearly, our choice of completely symmetric interaction parameters and compositions is not a generic case. If we simulate a quench with an off-critical composition

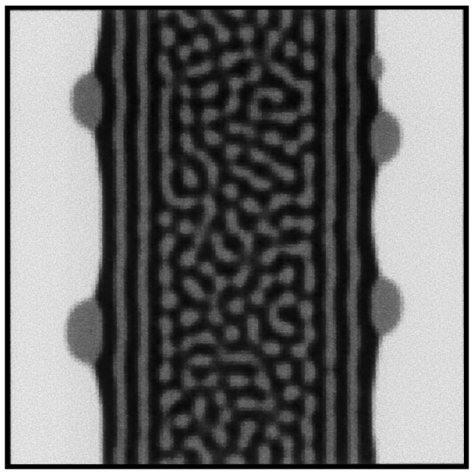

FIG. 2. Stripe of unstable material with asymmetric initial concentrations ($p^A = 0.56007$, $p^B = 0.37338$) at $\beta\varepsilon_{AA} = 2$ on a 128×128 lattice with periodic boundary conditions; $t = 89\,400 w_0^{-1}$.

ratio 60:40 (Fig. 2), we find spinodal waves as described previously [10,11]. The patterns in the interior of the sample are very similar to those found for a binary model near a flat wall [14], but the surface mode still shows up and destabilizes the first layer of the wave. Droplets form at the surface which coarsen very rapidly. Similar pictures arise when we choose slightly different interaction energies for the different species.

Finally, we want to address the question of the thickness d of the surface patterns. For both cases (checkerboard and stripes), it depends on the strength of the initial noise. This can be seen as follows. In view of the exponential growth (8), the time necessary for a well-defined structure to evolve is

$$\tau \approx (1/\omega) \ln(\delta/\delta_0), \tag{12}$$

where δ_0 is the initial noise strength, and δ is some threshold value where nonlinear effects start to limit the growth. We can estimate the ratio of bulk and surface growth rates by comparing the times after which surface and bulk structures begin to show up. We obtain a value near four, in good agreement with our estimates. Furthermore, the surface mode propagates with velocity v between times τ_s when it starts from the surface and τ_b when the growing bulk structures stop its advance. Hence we have for the thickness d:

$$d \approx v(\tau_b - \tau_s) \approx (1/c)(\omega_s/\omega_b - 1) \ln(\delta/\delta_0). \tag{13}$$

We see that d is a logarithmic function of the initial noise strength. This was confirmed by our simulations. This point could be relevant for experiments, because for rapid quenches the initial fluctuations are basically the equilibrium fluctuations of the stable parent phase, which depend on the temperature *before* the quench. Different initial temperatures should therefore cause variations in d, in contrast to bulk phase separation, where a change of the fluctuation strength simply renormalizes the time scale.

In summary, we have analyzed the effects of free surfaces on the spinodal decomposition of binary alloys with vacancies. In simulations, we obtained surface structures of different morphologies. Our mean-field method allows one to obtain good estimates of the involved characteristic length and time scales in terms of the microscopic model parameters. It would be interesting to compare these findings to Monte Carlo simulations and to experiments.

We thank W. Dieterich, H-P. Fischer, M. Kolb, and P. Maass for very interesting discussions. M. P. benefited from a grant by the Ministère de l'enseignement supérieur et de la recherche (MESR). Laboratoire de Physique de la Matière Condensée is Unité de Recherche Associée (URA) 1254 to CNRS.

[1] J. W. Cahn and J. E. Hilliard, J. Chem. Phys. **28**, 258 (1958).
[2] For a review, see A. J. Bray, Adv. Phys. **43**, 357 (1994), and references therein.
[3] R. A. L. Jones, L. J. Norton, E. J. Kramer, F. S. Bates, and P. Wiltzius, Phys. Rev. Lett. **66**, 1326 (1991).
[4] P. Wiltzius and A. Cumming, Phys. Rev. Lett. **66**, 3000 (1991).
[5] A. Cumming, P. Wiltzius, F. S. Bates, and J. H. Rosedale, Phys. Rev. A **45**, 885 (1992).
[6] F. Bruder and R. Brenn, Phys. Rev. Lett. **69**, 624 (1992).
[7] B. Q. Shi, C. Harrison, and A. Cumming, Phys. Rev. Lett. **70**, 206 (1993).
[8] M. Kolb, T. Gobron, J.-F. Gouyet, and B. Sapoval, Europhys. Lett. **11**, 601 (1990).
[9] C. Sagui, A. M. Somoza, C. Roland, and R. C. Desai, J. Phys. A **26**, L1163 (1993).
[10] S. Puri and K. Binder, Phys. Rev. E **49**, 5359 (1994).
[11] H. L. Frisch, P. Nielaba, and K. Binder, Phys. Rev. E **52**, 2848 (1995).
[12] P. Keblinski, S. K. Kumar, A. Maritan, J. Koplik, and J. R. Banavar, Phys. Rev. Lett. **76**, 1106 (1996).
[13] H.-P. Fischer, P. Maass, and W. Dieterich (unpublished).
[14] C. Geng and L.-Q. Chen, Surf. Sci. **355**, 229 (1996).
[15] K. Yaldram and K. Binder, Acta Metall. **39**, 707 (1990); J. Stat. Phys. **62**, 161 (1991); Z. Phys. B **82**, 405 (1991).
[16] C. Frontera, E. Vives, and A. Planes, Phys. Rev. B **48**, 9321 (1993).
[17] P. Fratzl and O. Penrose, Phys. Rev. B **50**, 3477 (1994).
[18] C. Geng and L.-Q. Chen, Scr. Metall. Mater. **31**, 1507 (1994).
[19] A. G. Khatchaturyan, Sov. Phys. Solid State **9**, 2040 (1968).
[20] L.-Q. Chen, Acta Metall. Mater. **42**, 3503 (1994).
[21] V. Y. Dobretsov, V. G. Vaks, and G. Martin, Phys. Rev. B **54**, 3227 (1996).
[22] M. Plapp and J.-F. Gouyet, Phys. Rev. E **55**, 45 (1997); **55**, 5321 (1997).
[23] W. W. Mullins and R. F. Sekerka, J. Appl. Phys. **3**, 444 (1964).